Weierstraß-Institut
für Angewandte Analysis und Stochastik

im Forschungsverbund Berlin e.V.

Preprint ISSN 0946 – 8633

Second order accurate explicit finite volume schemes for the solution of Boltzmann-Peierls equation

Wolfgang Dreyer, Shamsul Qamar

submitted: 27th August 2003

Weierstrass Institute
for Applied Analysis
and Stochastics
Mohrenstrasse 39
10117 Berlin
Germany
E-Mail: dreyer@wias-berlin.de
qamar@wias-berlin.de

No. 860
Berlin 2003

2000 *Mathematics Subject Classification.* 65M99, 76Y05, 80A99, 76M12, 35L15.

Key words and phrases. Boltzmann-Peierls equation, heat transfer, hyperbolic moment system, Bose-gas, phonons, upwind schemes, central schemes, high order accuracy.

Edited by
Weierstraß-Institut für Angewandte Analysis und Stochastik (WIAS)
Mohrenstraße 39
D — 10117 Berlin
Germany

Fax: + 49 30 2044975
E-Mail: preprint@wias-berlin.de
World Wide Web: http://www.wias-berlin.de/

Abstract

In this article we present the first and second order numerical schemes for the solution of initial value problems of the Boltzmann-Peierls equation (BPE). We also modify the numerical schemes for the solution of initial and boundary value problems (IBVP) of its derived hyperbolic moment system. BPE is an integro-differential equation which describes the evolution of heat in crystalline solids at very low temperatures. The BPE describes the evolution of the phase density of a phonon gas. The corresponding entropy density is given by the entropy density of a Bose-gas. We derive a reduced three-dimensional kinetic equation which has a much simpler structure than the original BPE, while it still retain all the properties of the original BPE. Using special coordinates, we get a further reduction of the kinetic equation in one space dimension. We introduce the discrete-velocity model of the reduce BPE in one space dimension. This discrete-velocity model can be discretized in space and time by using finite volume schemes. We derive both first and second order explicit upwind and central schemes for the discrete-velocity kinetic equation as well as for the derived moment system. We use the kinetic approach in order to prescribe boundary conditions for the IBVP of the moment system. Several numerical test cases are considered in order to validate the theory.

1 Introduction

The Boltzmann equation is the basic model in the kinetic theory of gases. Boltzmann-type equations are also involved in modelling electron transport in solids and plasma, neutron transport in nuclear reactors, radioactive transfer in planetary and stellar atmosphere, and heat transport in crystalline solids.

In 1929, Peierls [19] proposed his celebrated theoretical model based on the Boltzmann equation. According to him the lattice vibrations responsible for the heat transport can be described as an interacting gas of phonons. The Boltzmann-Peierls approach is one of the milestones of the theory of thermal transport in solids, especially at very low temperatures. It is important to mention that Fourier theory of heat flow fails to describe heat conduction processes at low temperatures, see for example Dreyer and Struchtrup [8] and references therein.

When solving the models like BGK or BPE, the main difficulty is the velocity discretization. Most numerical methods like Issautier [10], Aoki et al. [1], and Yang [23] have lacking to satisfy the conservation laws and entropy inequality. This leads to algorithms which are expensive due to the fine velocity mesh which guarantee robustness, in particular with implicit schemes.

An elegant approach which allows to have conservation and entropy properties with Boltzmann equation approximations is the discrete kinetic theory. It has been widely developed by Gatignol [9] who constructed some discrete velocity models (DVM) of Boltzmann equation. In addition, she demonstrated conservation properties and some other interesting results. These models were initially used to simplify the mathematical study of the Boltzmann equation. However, the recent numerical methods developed by Buet [3] as well as Rogier and Schneider [21], also use the DVM with above mentioned properties. Mieussens [17] has used a similar approach to that of [3, 21] for the development of a DVM of the BGK equation. He proved that this discrete model satisfies the conservation laws for mass, momentum and energy, as well as entropy inequalty. He also proved the existence and uniqueness results for that model. He used the conservative explit finite volume scheme to approximate the solution of this DVM. This conservative model was found to be very economic as compared to the non conservative methods for which a large number of discrete velocities are needed to recover conservation properties.

In this paper we present a similar approach to that of [3, 17, 21] for the development of a DVM of the Boltzmann-Peierls equation (BPE). This model is a simplified model of the actual BPE due to the simplification of the collision term by Callawy [4, 8]. This model is very similar in shape to the BGK-model of the gas kinetic theory with a main difference of two collision operators. Despite of this simplicity it contains most of the basic properties such as conservation of energy and heat flux. Therefore like BGK-equation this type of equation can also be used for testing numerical methods for kinetic equations.

Dreyer, Herrmann and Kunik [6] have used a first order kinetic scheme in order to solve the macroscopically one-dimensional and microscopically two-dimensional BPE. While, Kunik, Qamar and Warnecke [14] have used the first order kinetic scheme for the solution of microscopically three-dimensional model of BPE in one space dimension. We have also used kinetic schemes in order to solve the ultra-relativistic Euler equations [12, 13, 15], which utilizes similar ideas of [6, 14]. Here we present the first order and second order explicit upwind scheme [17] and central schemes [11, 18, 16] in order to solve the initial value problems of microscopically three-dimensional discrete-velocity model of the BPE equations in one space dimension.

Heat conduction processes are usually described by a parabolic system. It results from a diffusion law, where the heat flux is proportional to the temperature gradient. That constitutive law implies the paradox of heat conduction whereupon heat may traverse a body with infinite speed. This fact is not acceptable from physical point of view. In most technical process, in particular at room temperature, those modes that propagate with infinite speed suffer a considerable damping and are thus not observable. However, there are cases where either the damping of heat pulses is quite low or where its travel distance is so small that the transit time is an observable quantity. In those cases the parabolic system has to be replaced by physically justified hyperbolic system of heat conduction. A comprehensive study of many phenomena which appear in the temperature range between $5^o K$ and $20^o K$ is described in [5, 8]. In that range heat conduction of crystalline solids must be considered as the motion of phonons which may interact with the lattice impurities and with each other. The articles [5, 8] report on special circumstances that are met in a quite pure crystal at not too low temperature. Here the state of crystal is sufficiently described by four thermodynamic fields as the basic variables. These are the energy density e, or the temperature T, and the heat flux $\mathbf{Q} = (Q^i)_{i=1,2,3}$. The resulting system of field equations is of the symetric hyperbolic type.

In this paper we also consider this system in one space dimension and solve it for IBVP. We apply the same schemes which we are using for the solution of BPE equation with some modifications. This nonlinear system consist of a conservation equation for the energy density e and a balance equation for the heat flux Q^i, and it is derived by averaging of the BPE. The closure problem is solved by the *Maximum Entropy Principle* [7]. The IBVP that uses exclusively prescirbed boundary data for the energy density e is solved by a kinetic approach. The kinetic representation of the IBVP reveal a peculiar phenomenon. The contributions to the solution are from intial data at the right of the wall, as well as the fields at the wall e_w and Q_w. However, only one of these quantities can be controlled in an experiment. To overcome this problem we use a continuity condition. It turns out that after short time energy and heat flux are related to each other according to the Rankine Hugoniot jump relations given in [7, 5].

The Boltzmann-Peierls equation is a kinetic equation for the phase density of phonons. This equation describes the evolution of the phase density $f(t, \mathbf{x}, \mathbf{k})$, where $f(t, \mathbf{x}, \mathbf{k}) d^3x d^3k$ is interpreted as the number of phonons at time t in an infinitesimally small phase cell element $d^3x d^3k$ centered at $(\mathbf{x}, \mathbf{k})$. Here $\hbar\mathbf{k}$ denote the momentum, $\mathbf{k}$ the phonon wave vector and $\hbar$ is Planck's constant, see [19, 8] for further details. The microscopically three dimensional Boltzmann-Peierls equation (BPE) can be written as

$$\frac{\partial f}{\partial t} + \frac{\partial \omega}{\partial k_k} \frac{\partial f}{\partial x^i} = \zeta(f)\,, \tag{1}$$

where ω is the phonon frequency, t is time, and ζ is the collision operator which will be defined below. In a real crystal there are three phonon modes and thus there are three phase densities corresponding to two transversal modes and one longitudinal mode. In [8] it is described that for simplicity one can replace the actual crystal by a so called *Debye solid*, which is characterized by a single mode only. In addition the assumed dispersion relation between the phonon frequency ω and the wave vector $\mathbf{k}$ is given by

$$\omega = c\,|\mathbf{k}|\,. \tag{2}$$

Here the Debye velocity c is related to mean of the two transveral and longitudinal sound speeds of the actual crystal. Thus the BPE is given by

$$\frac{\partial f}{\partial t} + c \frac{k^i}{|\mathbf{k}|} \frac{\partial f}{\partial x^i} = \zeta(f)\,. \tag{3}$$

The moments of the phase density f reflect the kinetic processes on the scale of continuum physics. The most important moments are

$$e(t,\mathbf{x}) = \hbar c \int_{-\infty}^{\infty} |\mathbf{k}|\, f(t,\mathbf{x},\mathbf{k})\, d^3k\,, \tag{4}$$

$$Q^i(t,\mathbf{x}) = \hbar c^2 \int_{-\infty}^{\infty} k^i f(t,\mathbf{x},\mathbf{k})\, d^3k\,, \tag{5}$$

$$N^{ij}(t,\mathbf{x}) = \hbar c \int_{-\infty}^{\infty} \frac{k^i k^j}{|\mathbf{k}|} f(t,\mathbf{x},\mathbf{k})\, d^3k\,, \quad i,j = 1,2,3\,. \tag{6}$$

The fields e, $\mathbf{Q} = (Q^1, Q^2, Q^3)$ and the Matrix $\mathbf{N} = (N^{ij})$ are the energy density, heat flux and momentum flux, respectively. Phonons are classified as Bose particles [19, 8], and the corresponding entropy density-entropy flux pair (h, φ) is given by

$$h(f) := y \int_{\mathbb{R}^3} \left[\left(1 + \frac{f}{y}\right) \ln\left(1 + \frac{f}{y}\right) - \frac{f}{y} \ln\left(\frac{f}{y}\right) \right] d^3k\,, \tag{7}$$

$$\varphi^i(f) := yc \int_{\mathbb{R}^3} \frac{k^i}{|\mathbf{k}|} \left[\left(1 + \frac{f}{y}\right) \ln\left(1 + \frac{f}{y}\right) - \frac{f}{y} \ln\left(\frac{f}{y}\right) \right] d^3k\,, \tag{8}$$

where $y = \frac{3}{8\pi^3}$, see [8] .

In contrast to the ordinary gas atoms, the phonons may interact by two different collision processes, called R- and N-processes. R-processes include interactions of phonons with lattice impurities which destroy the periodicity of the crystal, while N-processes can be interpreted as phonon-phonon interactions which are due to the deviations from harmonicity of the crystal forces. N-processes conserve both, energy and momentum, while R-processes only conserve energy. The Callaway approximation of the collision operator [4, 8] is a suitable simplification of the actual interaction processes. The Callaway collision operator is written as the sum of two relaxation operators modelling the R- and N-processes seperately. We write

$$\zeta(f) = \zeta_R(f) + \zeta_N(f)\,, \qquad \zeta_\alpha = \frac{1}{\tau_\alpha}\,(P_\alpha f - f)\;, \quad \alpha \in \{R, N\}\;. \tag{9}$$

The positive constants τ_R and τ_N are the relaxation times, while P_R and P_N are two nonlinear projectors. Here $P_R f$ and $P_N f$ represent the phase densities in the limiting case when the relaxation time tends to zero. Explicitly, we define $P_R f$ and $P_N f$ as the solutions of two optimization problems, namely

$$h(P_R f) = \max_{f'} \{h(f) \;:\; e(f') = e(f)\}\;, \tag{10}$$

$$h(P_N f) = \max_{f'} \{h(f) \;:\; e(f') = e(f),\, \mathbf{Q}(f') = \mathbf{Q}(f)\}\;, \tag{11}$$

where $e(f)$, $\mathbf{Q}(f)$ are given by (4), (5). The maximization problems can be solved by means of Lagrange multipliers Λ_R^0 and Λ_N^0, Λ_N^1, Λ_N^2, Λ_N^3. Therefore we get

$$P_R f(\mathbf{k}) = \frac{y}{-1+\exp(\Sigma_R)}\,, \qquad P_N f(\mathbf{k}) = \frac{y}{-1+\exp(\Sigma_N)}\,, \tag{12}$$

where

$$\Sigma_R(t,\mathbf{x},\mathbf{k}) = \hbar c\,|\mathbf{k}|\,\Lambda_R^0\,, \tag{13}$$

$$\Sigma_N(t,\mathbf{x},\mathbf{k}) = \hbar c\,|\mathbf{k}|\,\Lambda_N^0(t,\mathbf{x}) + \hbar\,k^i\,\Lambda_N^i(t,\mathbf{x})\,. \tag{14}$$

From (10) and (11) the Lagrange multipliers can be calculated explicitly. They are given by, see [5], [6],

$$\Lambda_R^0 = \left(\frac{10\hbar^3c^3}{\pi^2}e\right)^{-\frac{1}{4}}, \quad \Lambda_N^0 = \gamma\frac{\left(\frac{F}{e}\right)^{\frac{1}{4}}}{(4-F)^{\frac{3}{4}}}\,, \quad \Lambda_R^i = -\frac{\gamma}{4}\frac{\left(\frac{F}{e}\right)^{\frac{5}{4}}}{(4-F)^{\frac{3}{4}}}Q^i\,, \tag{15}$$

$$F = \frac{6}{1+\sqrt{1-\frac{3}{4}\left(\frac{|\mathbf{Q}|}{ce}\right)^2}}\,, \quad \gamma = \left(\frac{4\pi^5 y}{45\hbar^3c^3}\right)^{\frac{1}{4}}. \tag{16}$$

When the thermodynamic state is described by four fields e and Q^i only, then we can derive the following balance equations from the Boltzmann-Peierls equation (3) and the maximum entropy principle, see [5],

$$\begin{aligned}
\frac{\partial e}{\partial t} + \frac{\partial Q^i}{\partial x^i} &= 0\,,\\
\frac{\partial Q^i}{\partial t} + \frac{\partial\left(c^2N^{ij}\right)}{\partial x^j} &= -\frac{1}{\tau_R}Q^i\,, \quad i,j=1,2,3,\\
N^{ij} &= \frac{1}{3}e\,\delta^{ij} + \frac{1}{2}e(3\chi-1)\left(\frac{Q^iQ^j}{|\mathbf{Q}|^2}-\frac{1}{3}\delta^{ij}\right),
\end{aligned} \tag{17}$$

where χ is the so called Eddington-factor:

$$\chi = \frac{5}{3} - \frac{4}{3}\sqrt{1-\frac{3}{4}\left(\frac{|\mathbf{Q}|}{ce}\right)^2}\,. \tag{18}$$

Note that in above equations (17) the τ_N term do not appear on the right hand side, therefore the applicability of these equations is restricted to the relaxation limit $\tau_N \to 0$.

Taking the integral-moments of the BPE, one can generate an infinite number of further balance equations, because there follows for any vector $\mathbf{m}(\mathbf{n})$ of moment weights

$$\frac{\partial \mathbf{u}(f)}{\partial t} + \frac{\partial \mathbf{F}^i(f)}{\partial x^i} = \mathbf{u}(\zeta(f))\,, \qquad i=1,2,3. \tag{19}$$

Here, $\mathbf{u}$ and $\mathbf{F}^i$ are the vectors of densities and fluxes, respectively. They are defined as

$$\mathbf{u}(f) = \int_{\mathbb{R}^3} \mathbf{m}(\mathbf{k})f(\mathbf{k})\,d^3k\,, \qquad \mathbf{F}^i(f) = \int_{\mathbb{R}^3} \frac{k^i}{|\mathbf{k}|}\,\mathbf{m}(\mathbf{k})f(\mathbf{k})\,d^3k\,. \tag{20}$$

Furthermore, the kinetic equation (3) implies an entropy inequality, i.e., any solution f of (3) satisfies

$$\frac{\partial h(f)}{\partial t} + \frac{\partial \varphi^i(f)}{\partial x^i} \geq 0\,. \tag{21}$$

It is well known that the balance-laws (19) can be reduced to a hyperbolic moment system by using the maximum entropy principle like in (10), (11) and (17)-(18), see [6].

This paper consist of seven sections. In Section 2, we recall the three-dimensional original BPE and derive a reduced kinetic equation for a reduced kinetic phase density, see [6, 14]. Moreover, we give a reduced form of the reduced entropy density-entropy flux pair. In Section 3, we introduce one-dimensional reduced BPE. Using special coordinates, we futher reduce the already reduced BPE in one space dimension. We then replace this reduced BPE by a discrete-velocity model. In Section 4, we solve this discrete-velocity model by first and second order explicit upwind and cenral schemes. In Section 5, we introduce the one-dimensional hyperbolic moment system [5, 8]. We modify our numerical schemes for the solution of the initial and boundary value problems of the moment system. In order to calaculte the force term we allow the phonon-phonon collisions at the cell interface. In section 6, we present some numerical test case computations for both BPE and its hyperbolic moment system. In Section 7, we give the conclusion of the results and future recommendations.

2 Reduced Boltzmann-Peierls Equation

In this section we intend to recall results from [6, 14] in order to derive a reduced kinetic equation for a reduced phase density. This procedure relies on the observation that for any solution f of (3) there exists a corresponding solution of a reduced equation that determines all physically important moments of f. Additionally we give the expression for the reduced entropy density-entropy flux pair, as it was done in [6, 14].

The phase density f depends on the wave vector $\mathbf{k} \in \mathbb{R}^3$, therefore we can calculate the reduced phase density according to the radial integration in polar-coordinates:

$$\Psi(\mathbf{n}) = \hbar c \int_0^\infty |\mathbf{k}|^3 \, f(|\mathbf{k}|\, \mathbf{n}) \, d|\mathbf{k}|\,. \tag{22}$$

Note that Ψ only depends on the unit vector $\mathbf{n} = (n^1, n^2, n^3) = \dfrac{\mathbf{k}}{|\mathbf{k}|}$.

Let m be a homogeneous moment weight of degree 1, i.e. $m(\lambda \mathbf{k}) = \lambda m(\mathbf{k})$ for all $\lambda \geq 0$.

Also let $\mathbf{u}$ be the corresponding moment function, then we have

$$\mathbf{u}(f) = \hbar c \int\limits_{\mathbb{R}^3} m(\mathbf{k}) f(\mathbf{k})\, d\mathbf{k} = \hbar c \oint\limits_{\partial B(0,1)} \int\limits_0^\infty |\mathbf{k}|^3\, m(\mathbf{n}) f(|\mathbf{k}|\,\mathbf{n})\, d|\mathbf{k}|\, dS(\mathbf{n}) \tag{23}$$

$$= \oint\limits_{\partial B(0,1)} m(\mathbf{n}) \Psi(\mathbf{n})\, dS(\mathbf{n})\,. \tag{24}$$

The moment $\mathbf{u}$ of f is thus given by the corresponding moments of Ψ. All the moments with physical interpretation cf. (4), (5), (6) are formed by homogeneous moment weights of degree 1. In particular we have

$$e(f) = e(\Psi)\,, \quad Q^i(f) = Q^i(\Psi)\,, \quad N^{ij}(f) = N^{ij}(\Psi)\,, \tag{25}$$

where

$$e(\Psi) = \oint\limits_{\partial B(0,1)} \Psi(\mathbf{n})\, dS(\mathbf{n})\,, \quad Q^i(\Psi) = c \oint\limits_{\partial B(0,1)} n^i \Psi(\mathbf{n})\, dS(\mathbf{n})\,, \tag{26}$$

$$N^{ij}(\Psi) = \oint\limits_{\partial B(0,1)} n^i n^j \Psi(\mathbf{n})\, dS(\mathbf{n})\,. \tag{27}$$

Similarly the reduced collision operators Φ, Φ_R and Φ_N are given by, see [6],

$$\Phi_\alpha = \frac{1}{\tau_\alpha} \left(\Theta_\alpha \Psi - \Psi\right)\,, \quad \alpha \in \{R, N\}\,, \quad \Phi = \Phi_R + \Phi_N\,, \tag{28}$$

where

$$\Theta_R \Psi = \frac{e}{4\pi}\,, \quad \Theta_N \Psi = \frac{3}{4\pi} \frac{e(4-F)^3}{F\left(1 - \frac{F\, n^i\, Q^i}{4\, c\, e}\right)^4}\,, \quad F = \frac{6}{1 + \sqrt{1 - \frac{3}{4}\left(\frac{|\mathbf{Q}|}{c\, e}\right)^2}}, \tag{29}$$

and

$$\hbar c \int\limits_0^\infty |\mathbf{k}|^3\, P_\alpha f(|\mathbf{k}|\,\mathbf{n})\, d|\mathbf{k}| = \Phi_\alpha(\mathbf{n}), \quad \alpha \in \{R, N\}\,. \tag{30}$$

We finally conclude that any solution $f(t, \mathbf{x}, \mathbf{k})$ of (3) induces a solution $\Psi(t, x, \mathbf{n})$ of the following reduced Boltzmann-Peierls equation

$$\frac{\partial \Psi}{\partial t}(t, \mathbf{x}, \mathbf{n}) + c\, n^i\, \frac{\partial \Psi}{\partial x^i}(t, \mathbf{x}, \mathbf{n}) = \Phi(t, \mathbf{x}, \mathbf{n})\,. \tag{31}$$

This reduced kinetic equation can be rewritten in the following time integral form by using Duhamel's principle

$$\Psi(t+\tau, \mathbf{x}, \mathbf{n}) = \Psi(t, \mathbf{x} - c\tau\mathbf{n}, \mathbf{n}) + \sum_{\alpha \in \{R,N\}} \int\limits_0^\tau \Phi_\alpha(s, \mathbf{x} - c(\tau - s)\mathbf{n}, \mathbf{n})\, ds\,, \tag{32}$$

where $\Psi(t, \mathbf{x} - c\tau\mathbf{n}, \mathbf{n})$ is the solution at time $t + \tau$ of the collisionless kinetic equation

$$\frac{\partial \Psi}{\partial t}(t, \mathbf{x}, \mathbf{n}) + c\, n^i \, \frac{\partial \Psi}{\partial x_i}(t, \mathbf{x}, \mathbf{n}) = 0\,. \tag{33}$$

In particular, $\Psi_0(t, \mathbf{x} - c\tau\mathbf{n}, \mathbf{n})$ is the free-flight solution of (33) for initial data Ψ_0.

Finally we introduce an entropy density-entropy flux pair for the reduced equation (31). The definition is not so straight forward as before, because in general the entropy density $h(f)$ cannot be determined from Ψ. The following definition is proposed in [6]

$$h(\Psi) = \mu \oint\limits_{\partial B(0,1)} \Psi^{\frac{3}{4}}(\mathbf{n})\, dS(\mathbf{n})\,, \tag{34}$$

$$\varphi^i(\Psi) = \mu\, c \oint\limits_{\partial B(0,1)} n^i \, \Psi^{\frac{3}{4}}(\mathbf{n})\, dS(\mathbf{n})\,, \quad \mu = \frac{4\pi}{3}\left(\frac{y}{15}\right)^{\frac{1}{4}}\,, \quad y = \frac{3}{8\pi^3}\,. \tag{35}$$

It was shown in [6] that this entropy density definition for the transformed BPE leads to the same results of the original entropy density definition (7) for the original BPE.

3 One-dimensional Reduced Kinetic Equation

Here we are interested in further reduction of the already reduced continuous-velocity Boltzmann-Peierls equation (31), see [14]. Later on, we write the discrete-velocity form of this reduced equation.

In the one dimensional case we have $\mathbf{x} = (x, 0, 0)$, $\mathbf{Q} = (Q(t,x), 0, 0)$ and $e = e(t,x)$. We introduce the new variables $-1 \leq \xi \leq 1$, $0 \leq \vartheta \leq 2\pi$ by

$$n^1 = \xi\,, \qquad n^2 = \sqrt{1-\xi^2}\sin\vartheta\,, \qquad n^3 = \sqrt{1-\xi^2}\cos\vartheta\,, \tag{36}$$

with the surface element $dS(\mathbf{n}) = d\xi d\vartheta$. Since in the one dimensional case the macroscopic fields inside the phase density $\Psi(t,x,\mathbf{n})$ will not depend on the angle ϑ, we can further reduce Ψ to

$$\psi(t,x,\xi) = \int_0^{2\pi} \Psi(t,x,0,0,\mathbf{n})\, d\vartheta = 2\pi\Psi(t,x,\xi). \tag{37}$$

The reduced Boltzmann-Peierls equation(31) then further reduces to

$$\frac{\partial \psi}{\partial t}(t,x,\xi) + c\,\xi\, \frac{\partial \psi}{\partial x}(t,x,\xi) = \sum_{\alpha\in\{R,N\}} \frac{1}{\tau_\alpha}\left(\Theta_\alpha\psi - \psi\right)(t,x,\xi)\,, \tag{38}$$

where

$$\Theta_R\psi = \frac{e}{2}\,, \quad \Theta_N\psi = \frac{3}{2}\frac{e(4-F)^3}{F\left(1-\frac{F\,\xi\,Q}{4\,c\,e}\right)^4}\,, \quad F = \frac{6}{1+\sqrt{1-\frac{3}{4}\left(\frac{Q}{c\,e}\right)^2}}\,. \tag{39}$$

We have used the same notation for the projection as in (29), but this will not lead to confusion within the context. Also the reduced moments integrals are given by

$$e(t,x) = \int_{-1}^{1} \psi(t,x,\xi)\, d\xi, \quad Q(t,x) = c\int_{-1}^{1} \xi\psi(t,x,\xi)\, d\xi\,, \tag{40}$$

$$N(t,x) = N_{11}(t,x) = \int_{-1}^{1} \xi^2\psi(t,x,\xi)\, d\xi. \tag{41}$$

In our paper [14] we have shown by three lemmas that the above reduction is valid for all later times.

Discrete-Velocity Model of the Equation

Let us discretize the continuous $\xi - velocity$ in to discrete velocity set of the form

$$\mathcal{N} = \{\xi_m = -1 + m\Delta\xi, m = 1,2,3,...,N_\xi\}\,, \tag{42}$$

where N_ξ is the number of discretizations of ξ-velocity and $\Delta\xi = \frac{2}{N_\xi}$. Then we can replace the "continuous" velocity distribution functions $\psi(t,x,\xi)$ and $\Theta_\alpha\psi(t,x,\xi)$ by N_ξ vectors of the form $\psi_m(t,x) = \psi(t,x,\xi_m)$ and $\Theta_\alpha\psi_m(t,x) = \Theta_\alpha\psi(t,x,\xi_m)$. Therefore the discrete-velocity model of the above reduced BPE is given by

$$\frac{\partial\psi_m}{\partial t}(t,x) + c\,\xi_m\,\frac{\partial\psi_m}{\partial x}(t,x) = \sum_{\alpha\in\{R,N\}} \frac{1}{\tau_\alpha}\left(\Theta_\alpha\psi_m - \psi_m\right)(t,x)\,, \quad m\in\mathcal{N}\,, \tag{43}$$

where for $\psi_m = \psi_m(t,x)$

$$\Theta_R\psi_m = \frac{e}{2}\,, \quad \Theta_N\psi_m = \frac{3}{2}\frac{e(4-F)^3}{F\left(1-\frac{F\,\xi_m\,Q}{4\,c\,e}\right)^4}\,, \quad F = \frac{6}{1+\sqrt{1-\frac{3}{4}\left(\frac{Q}{c\,e}\right)^2}}\,. \tag{44}$$

The reduced moments integrals are then replaced by Riemann sum

$$e(t,x) = \Delta\xi\sum_{m=1}^{N_\xi}\psi_m(t,x)\,, \quad Q(t,x) = c\Delta\xi\sum_{m=1}^{N_\xi}\xi_m\psi_m(t,x)\,, \tag{45}$$

$$N(t,x) = N_{11}(t,x) = \Delta\xi\sum_{m=1}^{N_\xi}\xi_m^2\psi_m(t,x)\,. \tag{46}$$

4 Numerical Schemes for the Reduced BPE

Here we present the upwind and central schemes for the reduced BPE in one space dimension. However the extension of the schemes to multi-dimensional case is analogous.

4.1 Upwind Finite Volume Schemes

First order Scheme:

Let us consider a spatial grid defined by nodes $x_i = i\Delta x$ and cells $I_i = \left[x_{i-\frac{1}{2}}, x_{i+\frac{1}{2}}\right]$. Consider also a time discretization with $t_n = n\Delta t$. Let $\psi^n_{m,i} = \psi_m(t_n, x_i)$ and $\Theta_\alpha \psi^n_{m,i} = \Theta_\alpha \psi_m(t_n, x_i)$, $\alpha \in \{R, N\}$, be the corresponding discrete average values of the phase density $\psi_m(t_n, x)$ and equilibrium phase densities $\Theta_\alpha \psi_m(t_n, x)$ in each cell I_i at time t_n, respectively. Then the transport part of (43) is simply the linear convection equation, and can be approximated by a standered upwind finite volume scheme. For the nonlinear relaxation term, a standered centered approximation technique is used, see [17]. Our scheme thus reads

$$\psi^{n+1}_{m,i} = \psi^n_{m,i} - \lambda\left(\mathcal{F}^n_{m,i+\frac{1}{2}} - \mathcal{F}^n_{m,i-\frac{1}{2}}\right) + \Delta t\, \mathcal{S}^n_{m,i}\,, \tag{47}$$

where $\lambda = \frac{\Delta t}{\Delta x}$, and for the CFL condition $\Delta t \leq \frac{\Delta x}{2}$ we have

$$\mathcal{S}^n_{m,i} = \sum_{\alpha \in R,N} \frac{1}{\tau_\alpha}\left(\Theta_\alpha \psi^n_{m,i} - \psi^n_{m,i}\right)\,, \quad \mathcal{F}^n_{m,i+\frac{1}{2}} = \frac{c}{2}\left(\xi_m \psi^n_{m,i} + \xi_m \psi^n_{m,i+1} - |\xi_m| \Delta \psi^n_{m,i}\right)\,, \tag{48}$$

where $\Delta \psi^n_{m,i} = \xi_m \psi^n_{m,i+1} - \xi_m \psi^n_{m,i}$. In order to get the average values of the moments from this discrete phase density at any time t_n in each cell I_i we use the Riemann sums (45) and (46) as

$$e^n_i = \Delta\xi \sum_{m=1}^{N_\xi} \psi^n_{m,i}, \quad Q^n_i = c\Delta\xi \sum_{m=1}^{N_\xi} \xi_m \psi^n_{m,i}, \quad N^n_i = \Delta\xi \sum_{m=1}^{N_\xi} \xi^2_m \psi^n_{m,i}\,. \tag{49}$$

Second Order Extension of the Scheme:

For the second order accuracy in space and time we have the following three steps.

(I): **Data Reconstruction.** Starting with a piecewise-constant solution in time and space, $\sum \psi^n_{m,i}\chi_i(x)$, one reconstruct a piecewise linear (MUSCL-type) approximation in space, namely

$$\psi^n_m(x) = \sum \left[\psi^n_{m,i} + \psi^x_{m,i}\frac{(x - x_i)}{\Delta x}\right]\chi_i(x)\,. \tag{50}$$

Here, $\chi_i(x)$ is the characteristic function of the cell, $I_i := \{\eta \mid |\eta - x_i| \leq \frac{\Delta x}{2}\}$, centered arround $x_i = i\Delta x$, and $\psi^x_{m,i}$ abbreviates a first order discrete slope.

The extreme points $x = 0$ and $x = \Delta x$, in local coordinates correspond to the intercell boundaries in general coordinates $x_{i-\frac{1}{2}}$ and $x_{i+\frac{1}{2}}$, respectively, see Figure 1. The values of $\psi_{m,i}$ at the extreme points are

$$\psi^L_{m,i} = \psi^n_{m,i} - \frac{1}{2}\psi^x_{m,i}\,, \quad \psi^R_{m,i} = \psi^n_{m,i} + \frac{1}{2}\psi^x_{m,i}\,, \tag{51}$$

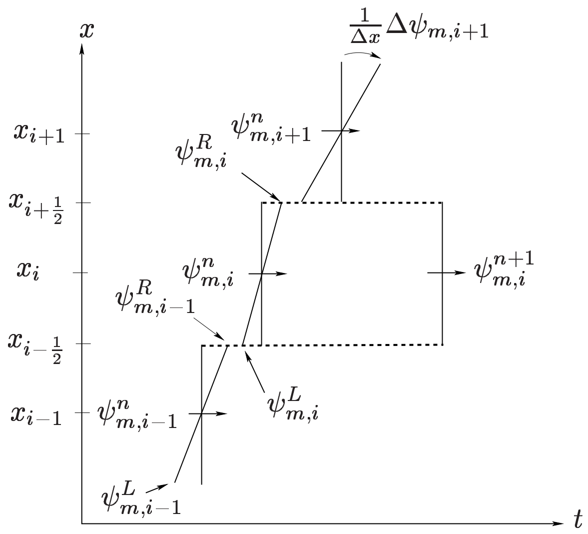

Figure 1: Second order reconstruction

and are usually called *boundary extrapolated values*.

A possible computation of these slopes, which results in an overall non-oscillatory schemes (consult [22]), is given by family of *discrete derivatives* parameterized with $1 \le \theta \le 2$, i.e., for any grid function $\psi_{m,i}$ we set

$$\psi^x_{m,i} = MM\left(\theta\Delta\psi_{m,i+\frac{1}{2}}, \frac{\theta}{2}(\Delta\psi_{m,i-\frac{1}{2}} + \Delta\psi_{m,i+\frac{1}{2}}), \theta\Delta\psi_{m,i-\frac{1}{2}}\right).$$

Here, Δ denotes the forward differencing, $\Delta\psi_{m,i+\frac{1}{2}} = \psi_{m,i+1} - \psi_{m,i}$, and MM denotes the min-mod nonlinear limiter

$$MM\{x_1, x_2, ...\} = \begin{cases} \min_i\{x_i\} & \text{if } x_i > 0 \quad \forall i\,, \\ \max_i\{x_i\} & \text{if } x_i < 0 \quad \forall i\,, \\ 0 & \text{otherwise}\,. \end{cases} \tag{52}$$

The interpolant (50), is then evolved exactly in time and projected on the cell-averages at the next time step.

(II): **Evolution.** For each cell I_i, the boundary extrapolated values $\psi^L_{m,i}$, $\psi^R_{m,i}$ in (51) are evolved for a time $\frac{1}{2}\Delta t$ by

$$\begin{aligned} \hat{\psi}^L_{m,i} &= \psi^L_{m,i} - \frac{\lambda}{2}\left[\mathcal{F}^R_{m,i} - \mathcal{F}^L_{m,i}\right] + \frac{\Delta t}{2}\mathcal{S}^n_{m,i}\,, \\ \hat{\psi}^R_{m,i} &= \psi^R_{m,i} - \frac{\lambda}{2}\left[\mathcal{F}^R_{m,i} - \mathcal{F}^L_{m,i}\right] + \frac{\Delta t}{2}\mathcal{S}^n_{m,i}\,, \end{aligned} \tag{53}$$

where $\mathcal{F}^L_{m,i} = c\xi_m\psi^L_{m,i}$ and $\mathcal{F}^R_{m,i} = c\xi_m\psi^R_{m,i}$. Also to calculate source term at half time step we use

$$\hat{\psi}_{m,i} = \psi^n_{m,i} - \frac{\lambda}{2}\left[\mathcal{F}^n_{m,i+1} - \mathcal{F}^n_{m,i}\right] + \frac{\Delta t}{2}\mathcal{S}^n_{m,i}\,, \tag{54}$$

where $\mathcal{F}^n_{m,i} = c\xi_m \psi^n_{m,i}$ and

$$\hat{e}_i = \Delta\xi \sum_{m=1}^{N_\xi} \hat{\psi}_{m,i}, \quad \hat{Q}_i = c\Delta\xi \sum_{m=1}^{N_\xi} \xi_m \hat{\psi}_{m,i} \, . \tag{55}$$

(III): Finally we use the conservative formula (47) in order to get the discrete phase density at next time step

$$\psi^{n+1}_{m,i} = \psi^n_{m,i} - \lambda \left(\mathcal{F}_{m,i+\frac{1}{2}} - \mathcal{F}_{m,i-\frac{1}{2}} \right) + \sum_{\alpha \in R,N} \frac{\Delta t}{\tau_\alpha} \left(\Theta_\alpha \psi_m(\hat{e}_i, \hat{Q}_i) - \hat{\psi}_{m,i} \right) , \tag{56}$$

where the numerical fluxes are defined by

$$\mathcal{F}_{m,i+\frac{1}{2}} = \frac{c}{2} \left[\xi_m \hat{\psi}^R_{m,i} + \xi_m \hat{\psi}^L_{m,i+1} - |\xi_m| (\hat{\psi}^L_{m,i+1} - \hat{\psi}^R_{m,i}) \right] . \tag{57}$$

4.2 Central Schemes

Central schemes for the numerical solution of conservation laws have been widely developed in the last decade. The first prototype of such schemes is Lax-Friedrichs scheme. Such scheme is more dissipative than first order Godunov scheme, but it is certainly easier to implement, since it does not require the knowledge of the charactersitic decomposition of the system or the knowledge of the (exact or approximate) solution to the Riemann problem.

Second order central schemes on staggrered grid have been derived independently by Nessyahu and tadmor (NT) [18] for the one space dimension and by Jaing and Tadmor (JT) [11] for the two space dimensions. Both NT and JT schemes do not require the solution of the Riemann problem. These schemes are very simple and efficient. It provide sharp shock resolution and can be easily used for systems for which the charactersitic decomposition is not known. Only an estimate of the largest eigenvalue of the jacobian matrix is necessary, in order to satisfy a suitable CFL condition.

NT scheme is obtained by piecewise linear non-osicllatory reconstruction from cell averages, and by the mid-point rule to compute the time integrals. Forward Euler scheme is used to compute the predictor value of the fields at the node of the midpoint rule. A generalization of NT schemes to the sytems with source term can be easily obtained by including the effect of the source predictor, and by using a quadrature formula to approximate the source term, see Liotta et al. [16]. In this paper we apply the central scheme to solve the one-dimensional reduced BPE and its moment system.

First Order Central (Lax-Friedrichs) Scheme:

Let us consider a spatial grid defined by node $x_i = i\Delta x$ and cells $I_i = \left[x_{i-\frac{1}{2}}, x_{i+\frac{1}{2}} \right]$. Consider also a time discretization with $t_n = n\Delta t$. Let $\psi^n_{m,i} = \psi_m(t_n, x_i)$ and $\Theta_\alpha \psi^n_{m,i} = \Theta_\alpha \psi_m(t_n, x_i)$, $\alpha \in \{R, N\}$, be the corresponding discrete average values of the phase density $\psi_m(t_n, x)$ and equilibrium phase densities $\Theta_\alpha \psi_m(t_n, x)$ in each cell I_i at time t_n, respectively. The integration of the reduced BPE (43) over the control volume $[x_i, x_{i+1}] \times [t_n, t_{n+1}]$ gives the first order central scheme as

$$\psi^{n+1}_{m,i+\frac{1}{2}} = \frac{1}{2}\left(\psi^n_{m,i} + \psi^n_{m,i+1}\right) - \lambda\left(\mathcal{F}^n_{m,i+1} - \mathcal{F}^n_{m,i}\right) + \frac{\Delta t}{2}\left(\mathcal{S}^n_{m,i} + S^n_{m,i+1}\right) , \tag{58}$$

where the force $\mathcal{F}$ and the source $\mathcal{S}$ are given by

$$\mathcal{F}^n_{m,i} = c\xi_m \psi^n_{m,i} , \quad \mathcal{S}^n_{m,i} = \sum_{\alpha \in R,N} \frac{1}{\tau_\alpha}\left(\Theta_\alpha \psi^n_{m,i} - \psi^n_{m,i}\right) . \tag{59}$$

In order to get the moments from this discrete phase density at any time t_n we use the Riemann sums (49). Again the CFL condition is $\Delta t = \frac{\Delta x}{2}$.

Second Order Extension of the Scheme:

Starting with a piecewise-constant solution in time and space, one reconstruct a piecewise linear (MUSCL-type) approximation of the form (50). The integration of the reduced BPE (43) over the control volume $[x_i, x_{i+1}] \times [t_n, t_{n+1}]$ gives

$$\psi^{n+1}_{m,i+\frac{1}{2}} = \psi^n_{m,i+\frac{1}{2}} + \frac{\lambda}{\Delta t}\left(\int_{t_n}^{t_{n+1}} \mathcal{F}_{m,i}(t)dt - \int_{t_n}^{t_{n+1}} \mathcal{F}_{m,i+1}(t)dt\right) + \frac{1}{\Delta x}\int_{x_i}^{x_{i+1}}\int_{t_n}^{t_{n+1}} \mathcal{S}_m(t,x)\, dt\, dx , \tag{60}$$

where $\lambda = \frac{\Delta t}{\Delta x}$, and

$$\mathcal{S}_m(t,x) = \sum_{\alpha \in R,N} \frac{1}{\tau_\alpha}\left(\Theta_\alpha \psi_m(t,x) - \psi_m(t,x)\right) , \tag{61}$$

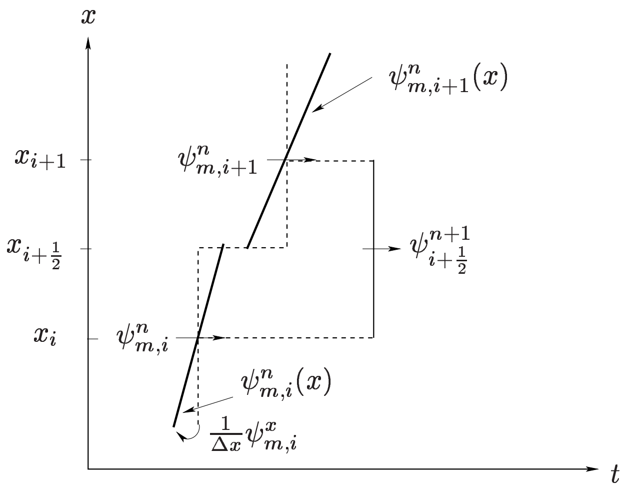

Figure 2: Second Order Reconstruction

The averaging of the linear data (50) at $t = t_n$, yields

$$\psi^n_{m,i+\frac{1}{2}} = \frac{1}{\Delta x}\int\limits_{x_i}^{x_{i+1}} \psi^n_m(x)dx$$

$$= \frac{1}{\Delta x}\left(\int\limits_{x_i}^{x_{i+\frac{1}{2}}} \psi^n_m(x)d\xi + \int\limits_{x_{i+\frac{1}{2}}}^{x_{i+1}} \psi^n_m(x)d\xi\right)$$

$$= \frac{1}{2}(\psi^n_{m,i} + \psi^n_{m,i+1}) + \frac{1}{8}(\psi^x_{m,i} - \psi^x_{m,i+1})\,. \tag{62}$$

The integral for the fluxes in (60) are discretized by midpoint rule. While for the integrals of the source term we use quadrature formula which is midpoint in time and trapezoidal rule in space. Thus we have

$$\int\limits_{t_n}^{t_{n+1}} \mathcal{F}_{m,i}(t)dt \sim \mathcal{F}^{n+\frac{1}{2}}_{m,i}\Delta t + O(\Delta t)^3\,. \tag{63}$$

$$\int\limits_{x_i}^{x_{i+1}}\int\limits_{t_n}^{t_{n+1}} \mathcal{S}_m(t,x)\,dtdx \sim \frac{1}{2}\left(\mathcal{S}^{n+\frac{1}{2}}_{m,i} + \mathcal{S}^{n+\frac{1}{2}}_{m,i+1}\right)\Delta t\Delta x + O(\Delta t)^3\,. \tag{64}$$

By Taylor expansion and BPE (43), we have

$$\psi^{n+\frac{1}{2}}_{m,i} = \psi^n_{m,i} + \frac{\Delta t}{2}(\psi^n_{m,i})_t + O(\Delta t)^2 = \psi^n_{m,i} - \frac{\lambda}{2}\mathcal{F}^x_{m,i} + \frac{\Delta t}{2}\mathcal{S}^n_{m,i} + O(\Delta t)^2\,. \tag{65}$$

This may serve as our approximate midvalues $\psi^{n+\frac{1}{2}}_{m,i}$ within the permissible second-order accuracy requirement. Here, $\frac{1}{\Delta x}\mathcal{F}^x_{m,i}$ stands for an approximate numerical derivatives of the flux $\mathcal{F}_{m,i}$,

$$\frac{1}{\Delta x}\mathcal{F}^x_{m,i} = \frac{\partial}{\partial x}\mathcal{F}_{m,i} + O(\Delta x)\,.$$

The fluxes $\mathcal{F}^x_{m,i}$ are computed by applying the min-mod limiter to each of the component of $\mathcal{F}$, i.e.,

$$\mathcal{F}^x_{m,i} = MM\left(\theta\Delta\mathcal{F}_{m,i+\frac{1}{2}}, \frac{\theta}{2}\left(\Delta\mathcal{F}_{m,i-\frac{1}{2}} + \Delta\mathcal{F}_{m,i+\frac{1}{2}}\right), \theta\Delta\mathcal{F}_{m,i-\frac{1}{2}}\right)\,.$$

Here, Δ denotes the forward differencing, $\Delta\mathcal{F}_{m,i+\frac{1}{2}} = \mathcal{F}_{m,i+1} - \mathcal{F}_{m,i}$, and MM denotes the min-mod nonlinear limiter given by (52).

In summary, this family of central differencing scheme takes the easily implemented predictor-corrector form,

$$\psi^{n+\frac{1}{2}}_{m,i} = \psi^n_{m,i} - \frac{\lambda}{2}\mathcal{F}^x_{m,i} + \frac{\Delta t}{2}\mathcal{S}^n_{m,i}\,, \tag{66}$$

$$
\begin{aligned}
\psi^{n+1}_{m,i+\frac{1}{2}} =& \frac{1}{2}(\psi^{n}_{m,i} + \psi^{n}_{m,i+1}) + \frac{1}{8}(\psi^{x}_{m,i} - \psi^{x}_{m,i+1}) \\
&+ \lambda \left(\mathcal{F}^{n+\frac{1}{2}}_{m,i} - \mathcal{F}^{n+\frac{1}{2}}_{m,i+1} \right) + \frac{\Delta t}{2} \left(\mathcal{S}^{n+\frac{1}{2}}_{m,i} + \mathcal{S}^{n+\frac{1}{2}}_{m,i+1} \right) .
\end{aligned}
\tag{67}
$$

In order to get the moments from this discrete phase density at any time t_n we use the Riemann sums (49).

5 Moment system of the One-Dimensional BPE

In this section we intend to solve the intial and boundary value problems of the moment system (17) of BPE in one-dimensional case. In this case the intial phase density at each time step is taken to be the eqilibrium phase density (44) of phonons $\Theta_N \psi$. In one dimensional case we can write (17) for $\tau_R \to \infty$ as

$$
\begin{aligned}
\frac{\partial e}{\partial t} + \frac{\partial Q}{\partial x} &= 0 , \\
\frac{\partial Q}{\partial t} + \frac{\partial \left(c^2 N\right)}{\partial x} &= 0 , \\
N = \frac{5}{3} e - \frac{4e}{3} & \sqrt{1 - \frac{3}{4}\left(\frac{Q}{ce}\right)^2} .
\end{aligned}
\tag{68}
$$

Given the piecewise constant initial data for the moments $e^n_i = e(t_n, x_i)$ and $Q^n_i = Q(t_n, x_i)$ at any time t_n in each cell I_i, we can calculate the intial phase density as $\psi^n_{m,i} = \Theta_N \psi^n_{m,i}$. The inital phase density at the next time step is obtained by using the conservative formula (47) with zero collision term, i.e,

$$
\psi^{n+1}_{m,i} = \psi^{n}_{m,i} - \lambda \left(\mathcal{F}^{n}_{m,i+\frac{1}{2}} - \mathcal{F}^{n}_{m,i-\frac{1}{2}} \right) , \tag{69}
$$

where $\lambda = \frac{\Delta t}{\Delta x}$. In order to add the phonon-phonon collisions to the collision-free phonon transport, we use the force term $\mathcal{F}$ as a convex combination of the form

$$
\mathcal{F}^{n}_{m,i+\frac{1}{2}} = (1-\eta) \mathcal{F}^{e}_{m,i+\frac{1}{2}} + \eta \mathcal{F}^{f}_{m,i+\frac{1}{2}} , \quad 0 \leq \eta \leq 1 . \tag{70}
$$

Here $\mathcal{F}^e$ is the equlibrium flux obtained from the equilibrium phase density $\Theta_N \psi$. While, $\mathcal{F}^f$ is free-flight (collision free) force terms. Here η is adjustable parameter. We have also used similar idea in [15] for the solution of the ultra-relativistic Euler equations. Theoritically, the parameter η should depend on the real flow situation: in equilibrium and smooth region, the use of $\eta \sim 0$ is physically resonable, and in discontinuity region, η should be close to 1 in order to have enough numerical dissipation to recover the smooth shock transition. A possible choice for η can be taken as a function of the energy density difference, such as the switch function in JST scheme. One possible choice for η can be

$$
\eta = 1 - \exp\left(-\alpha \frac{|e_l - e_r|}{e_l + e_r} \right) , \tag{71}
$$

where α is some constant and e_l and e_r are the energy density jump accross the the cell interface. If the natural CFL condition $\Delta t \leq \frac{\Delta x}{2}$ is satisfied, then

$$\mathcal{F}^{f}_{m,i+\frac{1}{2}} = \frac{c}{2}\left(\xi_m \psi^n_{m,i} + \xi_m \psi^n_{m,i+1} - |\xi_m| \Delta\psi^n_{m,i}\right) . \tag{72}$$

As a simple particle collisional model, we can imagin that the particles from the left- and right-hand sides of a cell interface collapse totally to form an equilibrium state. In order to define the equilibrium state at the cell interface, we need first to figure out the corresponding macroscopic quantitires $e^e_{\imath+\frac{1}{2}}$ and $Q^e_{\imath+\frac{1}{2}}$ there, which are the combination of the total energy and momentum of the left and right moving beams. Thus we have

$$e^e_{i+\frac{1}{2}}(t_n) = e^+_i(t_n) + e^-_{i+1}(t_n) , \qquad Q^e_{i+\frac{1}{2}}(t_n) = Q^+_i(t_n) + Q^-_{i+1}(t_n) , . \tag{73}$$

where for $\gamma^n_i = \frac{F^n_i Q^n_i}{4 c e^n_i}$ we obtain from (40)

$$e^{\pm}_i(t_n) = \frac{e^n_i}{2} \frac{(\gamma^n_i)^2 \mp 3\gamma^n_i + 3}{(\gamma^n_i)^2 + 3}(1 \pm \gamma^n_i)^3 , \quad Q^{\pm}_i(t_n) \quad = \frac{ce^n_i}{4} \frac{3 \mp \gamma^n_i}{(\gamma^n_i)^2 + 3}(\gamma^n_i \pm 1)^3 . \tag{74}$$

The "+" sign in (74) means that the integration limits for ξ in (40) are taken from 0 to 1, while the "−" sign means that the integration limits for ξ are ranging from -1 to 0. Thus we have

$$\mathcal{F}^e_{m,i+\frac{1}{2}} = c\xi_m \Theta_N \psi(t_n, e^e_{i+\frac{1}{2}} , Q^e_{i+\frac{1}{2}}) . \tag{75}$$

Using the relations (72) and (75) in conservative formula (69) we obtain the phase density at the next time step. Using the Riemann sums (49), we get the moments e^{n+1}_i and Q^{n+1}_i at the next time step. These moments are then used in the equilibrium phase density (44) in order to prepare the initial phase density for the next time step, i.e., $\psi^{n+1}_{m,i} = \Theta_N \psi(e^{n+1}_i, Q^{n+1}_i, \xi_m)$.

The procedure for the second order accuracy is exactly the same as given in the previous section. Also the modification of the central scheme for the moment system is just to neglect the collision term $\mathcal{S}$ in (66) and (67). Therefore we omit these discussions here.

5.1 Application of Boundary Conditions

Since we are using the conservative schemes, therefore the application of the boundary conditions is not complicated for the moment system. For the illustration of the boundary conditions we consider half space. We will discuss the boundary conditions only at the left boundary $x = 0$, however the procedure is similar for the other boundary and in multi-dimensional case. We consider the boundary $x = 0$ as a cell interface. We name the moments at the auxiliary cell I_A by e^n_A and on Q^n_A at the left of the boundary $x = 0$ at time t_n. We denote the values of the moments at the wall $x = 0$ by e^n_w and Q^n_w. Once we have the values of the moments at the auxiliary elements, we can calculate the equilibrium phase density at that element. According to (73) we have the conditions

$$e_w(t_n) = e^+_A(t_n) + e^-_1(t_n) , \qquad Q_w(t_n) = Q^+_A(t_n) + Q^-_1(t_n) , . \tag{76}$$

where $e^{\pm}$ and $Q^{\pm}$ can be obtained from (74) for a particular element. The fields e_1^n and Q_1^n on the right-hand side of the wall are known from the initial data. We have the following boundary conditions.

Reflecting Boundary Conditions

In this case we need the heat flux at the wall to be zero. Thus we take $e_A^n = e_1^n$ and $Q_A^n = -Q_1^n$, which is equivalent to $\psi_A(t_n, \xi_m) = \Theta_N \psi(e_1^n, |Q_1^n|, -\xi_m)$. This gives us the phase density at the auxiliary element for the reflecting boundary conditionas in our scheme.

Outflow Boundary Conditions

In this case we need the same values on both sides of the wall. Thus we take $e_A^n = e_1^n$ and $Q_A^n = Q_1^n$, which is equivalent to $\psi_A(t_n, \xi_m) = \Theta_N \psi(e_1^n, |Q_1^n|, \xi_m)$. This gives us the phase density at the auxiliary element for the outflow boundary condition.

Inflow Boundary Conditions

In this case if we are given the values of e_w^n and Q_w^n at the wall then we can use the equations (76) in order to find e_A^n and Q_A^n. However, in experimental point of view e_w^n and Q_w^n can not be given simultaneously. Either the energy density e_W^n is controlled at the wall, or the wall is equipped with a procedure of Joule's heat and thus the heat flux is prescribed. Here we consider the case that e_w^n is given from the experiment but not Q_w^n. It turns out that we require the continuity condition $e_A^n = e_w^n$ at each time step t_n. Using (74) we redefine

$$a^n = \frac{F_A^n Q_A^n}{4\, c\, e_A^n}\,, \qquad f(a^n) = \frac{1}{2}\,\frac{(a^n)^2 \mp 3a^n + 3}{(a^n)^2 + 3}(1 \pm a)^3\,,$$

then $(76)_1$ with $e_A^n = e_w^n$ gives

$$e_w^n = e_A^n f(a^n) + e_1^-(t_n)\,,$$

which implies

$$1 - f(a^n) = \frac{e_1^-(t_n)}{e_w^n}\,. \tag{77}$$

We know the right-hand side of this equation. Also f(a) is monotonically increasing with $f(-1) = 0$ and $f(1) = 1$, therefore the solution of the above equation only exist whenever the right-hand side is out of the range $[0, 1]$. We use Newton method to solve this equation for the unknown a^n. Finally we determine the auxiliary field Q_A^n according to

$$Q_A^n = \frac{4a^n}{(a^n)^2 + 3} e_A^n\,. \tag{78}$$

Once we have the auxiliary fields e_A^n and Q_A^n, then we can calculate the auxiliary phase density by $\psi_A(t_n, \xi_m) = \Theta_N \psi(e_1^n, Q_1^n, \xi_m)$.

6 Numerical Examples

In order to validate our results obtained in the previous sections, we present some numerical test cases. We consider the numerical test cases for the BPE, as well as for the hyperbolic moment system. The initial data in Subsections 6.1 – 6.2 are given for the BPE, while the IBVP data in Subsections 6.3 – 6.4 are given for the moment system.

6.1 Energy Pulse

Here we assume that $\tau_R = \infty$, so that from the physical point of view, we study a phonon gas in a pure crystal at low temperature. Since there are no lattice impurities, diffusion cannot appear. In particular, the propagation of heat behaves like a wave phenomenon. Further we assume that the phase density only depends on $x = x_1$. In order to simulate the problem for the BPE, we consider the following three types of macroscopic initial data for energy density e and the momentum density Q in the spatial domain $0 \leq x \leq 2$.

Problem 1:

The initial data are

$$e(0,x) = \begin{cases} 1.5 & \text{if} \quad 0.99 \leq x \leq 1.01 \\ 1.0 & \text{otherwise} \end{cases}, \qquad Q(0,x) = 0.0\,. \tag{79}$$

Furthermore, the Debye speed c is set to 0.5. We use $N_\xi = 200$ and $N_x = 100$, where N_ξ and N_x are the number of dicretizations in $\xi-$ and $x-$space.

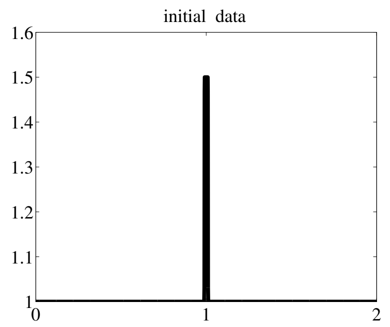

Figure 3: Initial energy pulse

Figures 4 shows the spatial dependence of the energy density, heat flux and momentum flux at different times for the relaxation time $\tau_N = 0.5$. While Figures 5 gives the distribution functions ψ and $\Theta_N\psi$ at time t=1.2.

Problem 2:

The initial data are

$$e(0,x) = 2.5e^{-40(x-1.0)^2}\,, \qquad Q(0,x) = 0.0\,, \tag{80}$$

where $c = 1.0$. We use $N_\xi = 200$ and $N_x = 100$. Figures 6 shows the spatial dependence of the energy density, heat flux and momentum flux at time $t = 0.5$.

Problem 3:

The initial data are

$$e(0,x) = 2 + \cos(4\pi x)\,, \qquad Q(0,x) = 0.0\,, \tag{81}$$

where $c = 1.0$. We use $N_\xi = 200$ and $N_x = 100$. Figures 7 shows the spatial dependence of the energy density, heat flux and momentum flux at time $t = 0.5$.

6.2 Two Interacting Heat Pulses

This test problem demonstrates the interaction of two heat pulses, which leads to a large increase of the energy density at the collision point during a short time interval. The initial data are

$$e(0,x) = \begin{cases} 1\,, & x \leq 0.3 \\ 2\,, & 0.3 \leq x \leq 0.4 \\ 1\,, & 0.4 \leq x \leq 0.6 \\ 2\,, & 0.6 \leq x \leq 0.7 \\ 1\,, & x \leq 1.0 \end{cases}, \quad Q(0,x) = \begin{cases} 0\,, & x \leq 0.3 \\ 1\,, & 0.3 \leq x \leq 0.4 \\ 0\,, & 0.4 \leq x \leq 0.6 \\ -1\,, & 0.6 \leq x \leq 0.7 \\ 0, & x \leq 1.0 \end{cases}. \tag{82}$$

We solve the BPE for the above problem at time $t = 0.2$ for two values of τ_N, i.e., $\tau_N = 1$ and $\tau_N = 0.1$, while $\tau_R = 1.0$. Figure 8 shows the results. From the comparison of the initial and final curves of energy density, we observe a large increase of the energy density e at the collision point $x = 0.5$.

6.3 Reflection of a Single Shock

Here consider a single shock solution for the moment system with reflecting boundary conditions at the lower boundary $x = 0$. The initial data are

$$(e,Q)(0,x) = \begin{cases} (1,0)\,, & x \leq 0.5\,, \\ \left(2, -\frac{1}{\sqrt{3}}\sqrt{\frac{3\sqrt{2}-1}{\sqrt{2}+1}}\right), & x \geq 0.5\,. \end{cases} \tag{83}$$

This single shock data was obtained in [7] by using Rankine-Hugoniot jump conditions. The computational domain is $0 \leq x \leq 1$. Here we take 200 discretizations in velcity ξ and 200 mesh points in $x-$space. Figure 9 show the results in time range $0 \leq t \leq 1.7$. While Figure 10 show the comparison of the results from upwind and central schemes at time $t = 1.7$. We take $\alpha = 1.0$ in equation (70) which is a collision-free transport at the cell interface.

6.4 Further Examples of IBVP for the Moment System

In the following numerical problems we apply the inflow boundary conditions to the moment system. We observe the following phenomena:

a) the formation and steeping of shock fronts,
b) the speed of shock front is apparently larger than $\frac{c}{\sqrt{3}}$,
c) the broadening of initial heat pulses at later times.

Test Case 1:

This problem represent the propagation of heat pulse

$$e_w(t) = \begin{cases} 1\,, & t \leq 0.0\,, \\ 3\,, & 0.0 < t \leq 0.5\,, \\ 1\,, & t > 0.5\,. \end{cases} \tag{84}$$

which is generated at lower boundary. The initial data are $e_0 = 1$ and $Q_0 = 0$, and the computational domain is $0 \leq x \leq 1.5$. Note that only $e_w(t)$ is prescribed, while $Q_w(t)$ is calculated according to (77) and (78). Figure 11 gives the results. The first row in Figure 11 show the boundary data, while the second row illustrate the solution at $t = 1.5$. We observe that the pulse front remains a shock moving with speed $0.72c$, which is confirmed by the shock conditions in [7]. The rear side of the pulse changes into rarefaction wave. We take $\alpha = 0.5$ in equation (70).

Test Case 2:

Here we create a periodic heat pulse

$$e_w(t) = 2 - \cos(8\pi t)\,, \tag{85}$$

at the lower boundary. The initial data are again $e_0 = 1$ and $Q_0 = 0$, and the computational doamin is $0 \leq x \leq 1.5$. Again $e_w(t)$ is prescribed but $Q_w(t)$ is calculated according to (77) and (78). Surprisingly even in this case $Q_w(t)$ meet the value which can be obtained by shock conditions in [7]. Figure 12 gives the results. The first row in Figure 12 show the boundary data, while the second row illustrate the solution at $t = 1.5$. The formation and steepening of shock fronts is clearly visible. We take $\alpha = 0.5$ in equation (70).

7 Conclusions

In this paper we have derived first- and second-order finite volume schemes for the solution of the reduced discrete velocity model of the Boltzmann-Peierls equations in one space dimension. The first reduction of the BPE reduces its moment integrals to surface integrals over the unit sphere. This reduction can be obtained without further assumptions on the initial data. Moreover we can obtained a second reduction of the already reduced BPE which is looking much simplier than the first one, but requires the additional assumption of a one-dimensional flow. Using special coordinates which when adapted for this one-dimensional flow, we can reduce the surface integrals for the moments to simple one-fold integrals ranging over the compact interaval -1 to 1. We have replaced this one-dimensional continuous-velocity BPE to a discrete-velocity model. This discrete-velocity model was then discretized in space and time by using explicit finite volume schemes. The numerical implementation of the first and second order upwind and central schemes for the initial value problems of the one-dimensional discrete-velocity model of BPE was found to be very simple due to the reduction of the actual BPE. However, the application of the boundary conditions for the BPE equation are complicated and need further study. On the other hand, we have solved the IBVP of the dervied hyperbolic four-field moment system. The application of the boundary conditions to the conservative schemes for the moment system are straightforward. We have used the kinetic approach in order to prescribe these boundary conditions. In experiments either energy density (temperature) or heat flux can be controlled on the boundary but not both simultaneously. To over come that problem we have used the continuity condition. Using that continuity condition and the initial data on the right of the wall we can easily obtain the other quantity. In this paper we have presented the case where the energy density is given at the wall but not the heat flux. It was found that after very short time the energy density and heat flux were related to each other according to Rankine Hugoniot Jump conditions, [7]. We have performed several numerical test case computations. It was found that the first order upwind scheme gives better resolution as compared to the first order central (Lax-Friedrichs) scheme. However, the second order central and upwind schemes have almost the same resolution. Both upwind and central schemes were found to be simple, compact, and easy to implement. The future tasks are the extension of the schemes to multi-dimensions and the application of the appropriate boundary conditions to the BPE.

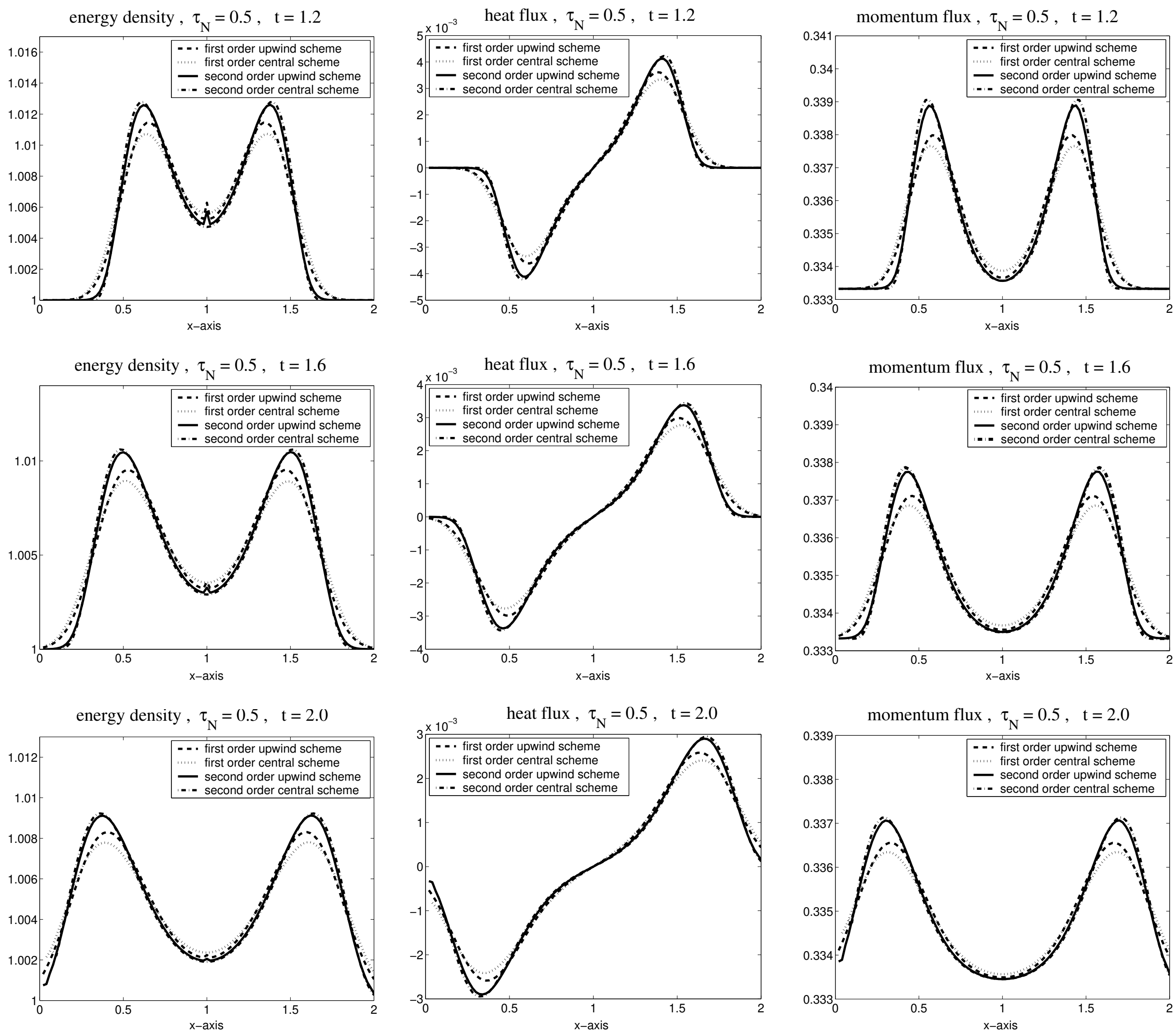

Figure 4: Evolution of enrgy, heat flux and momentum flux pulses at $\tau_N = 0.5$.

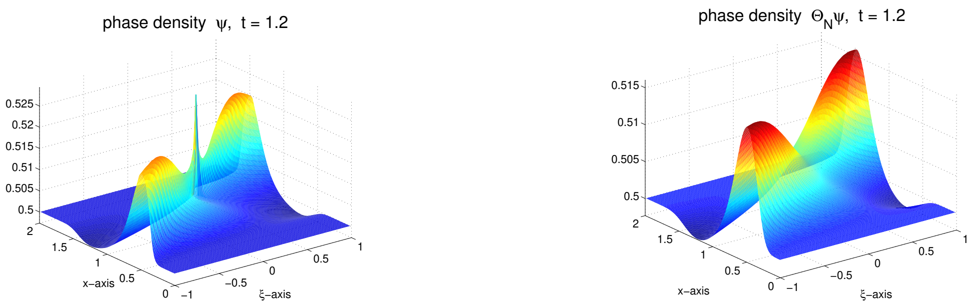

Figure 5: Representation of the phase densities at $\tau_N = 0.5$ and t=1.2.

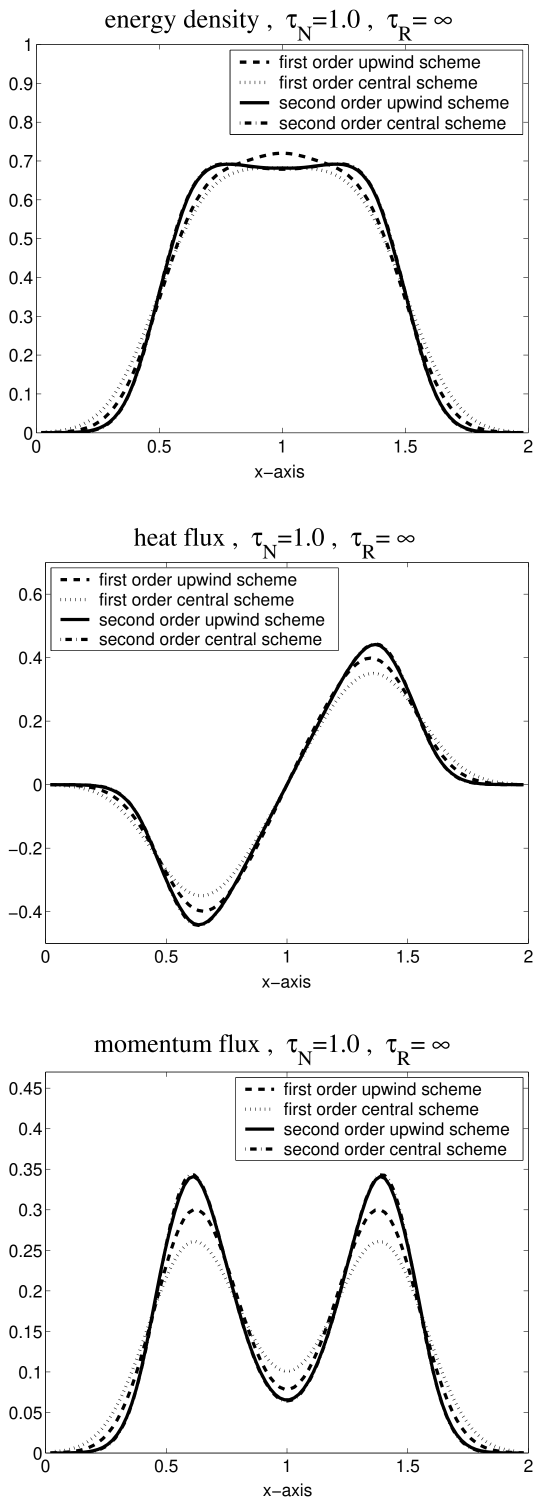

Figure 6: Evolution of energy and heat and momentum fluxes.

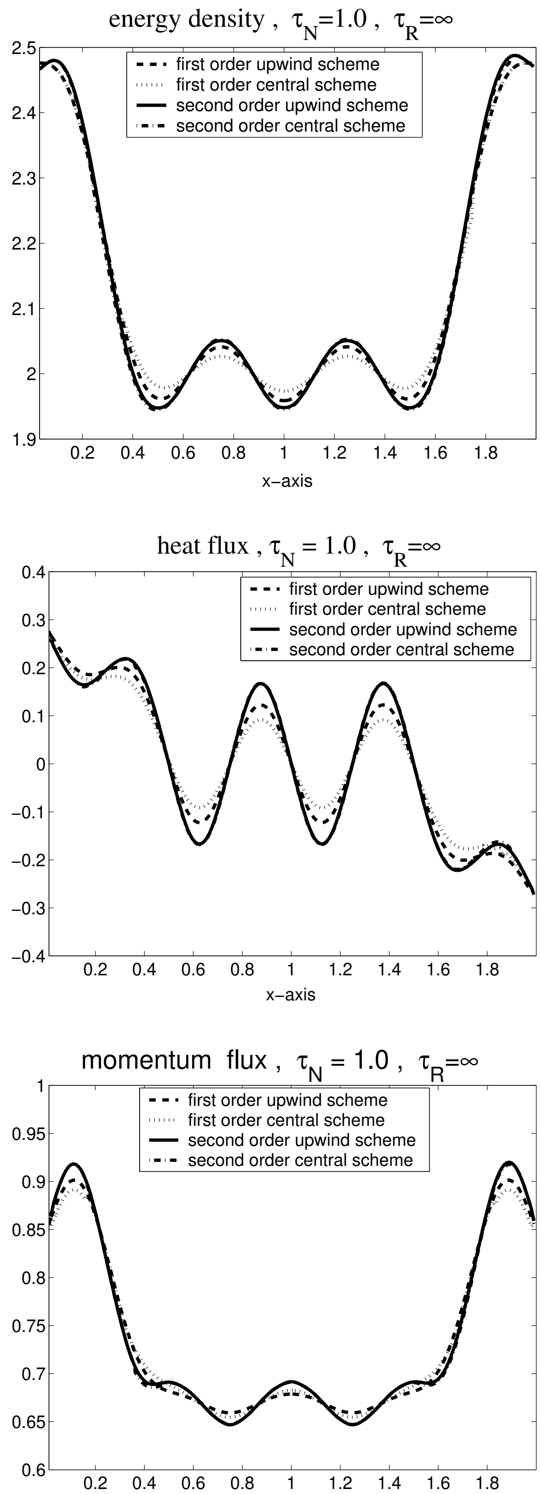

Figure 7: Evolution of energy density and heat flux.

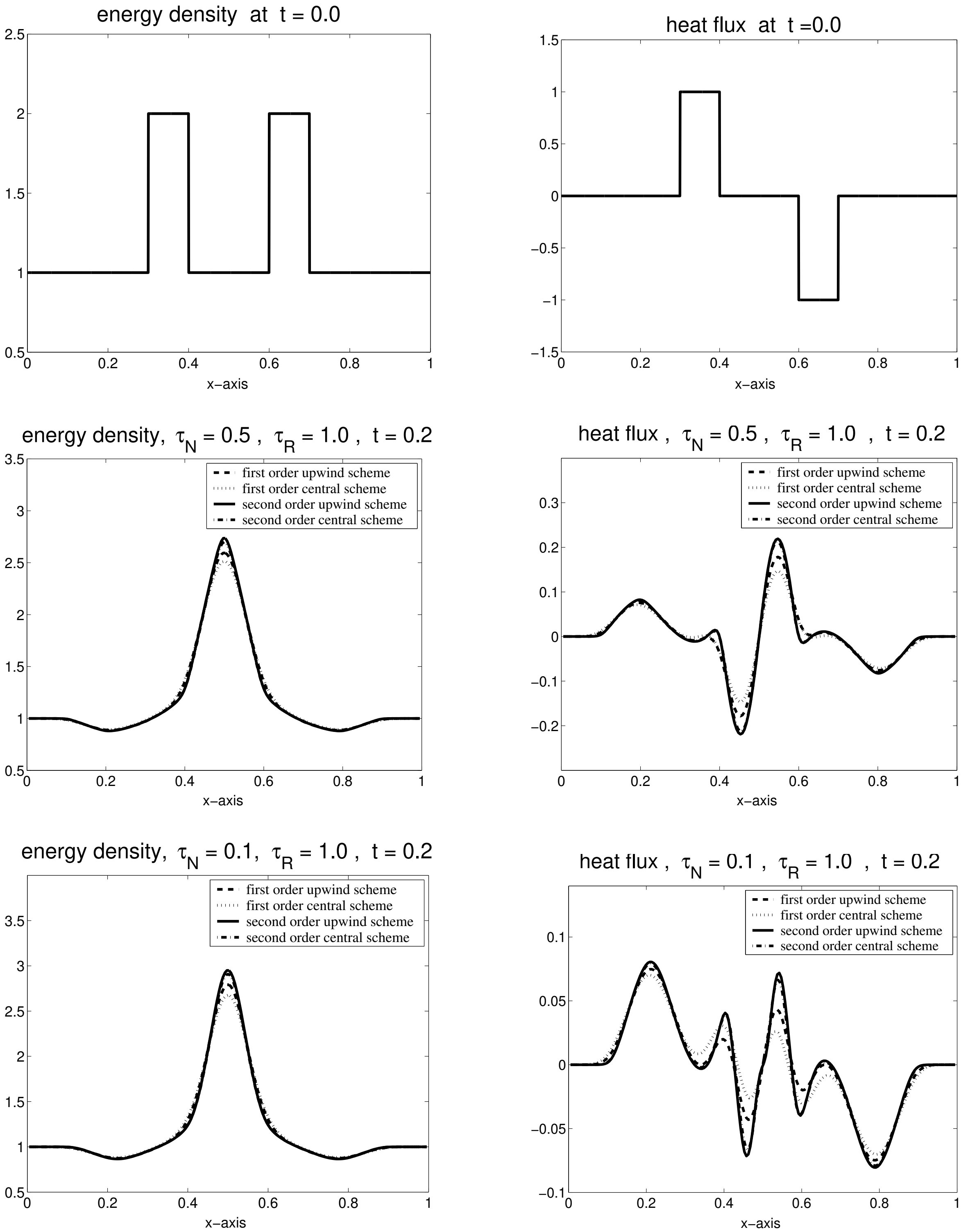

Figure 8: Evolution of energy and heat flux.

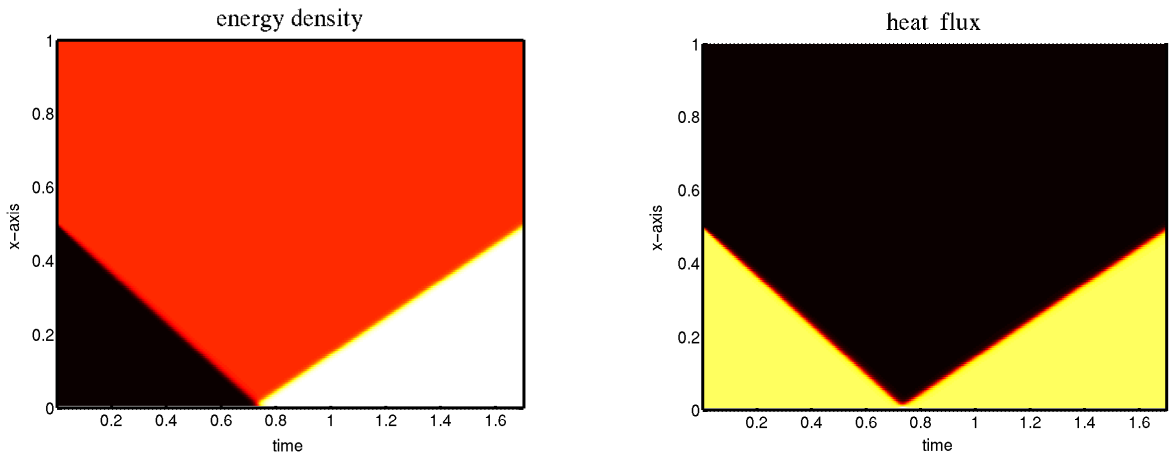

Figure 9: A single shock reflection using second order upwind scheme.

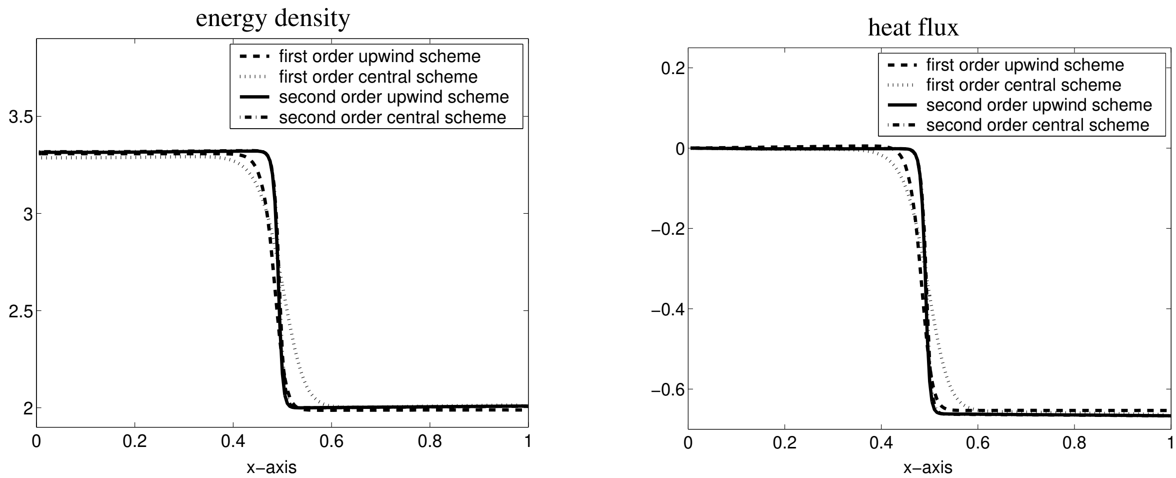

Figure 10: Comparison of schemes for a single shock reflection at t=1.7.

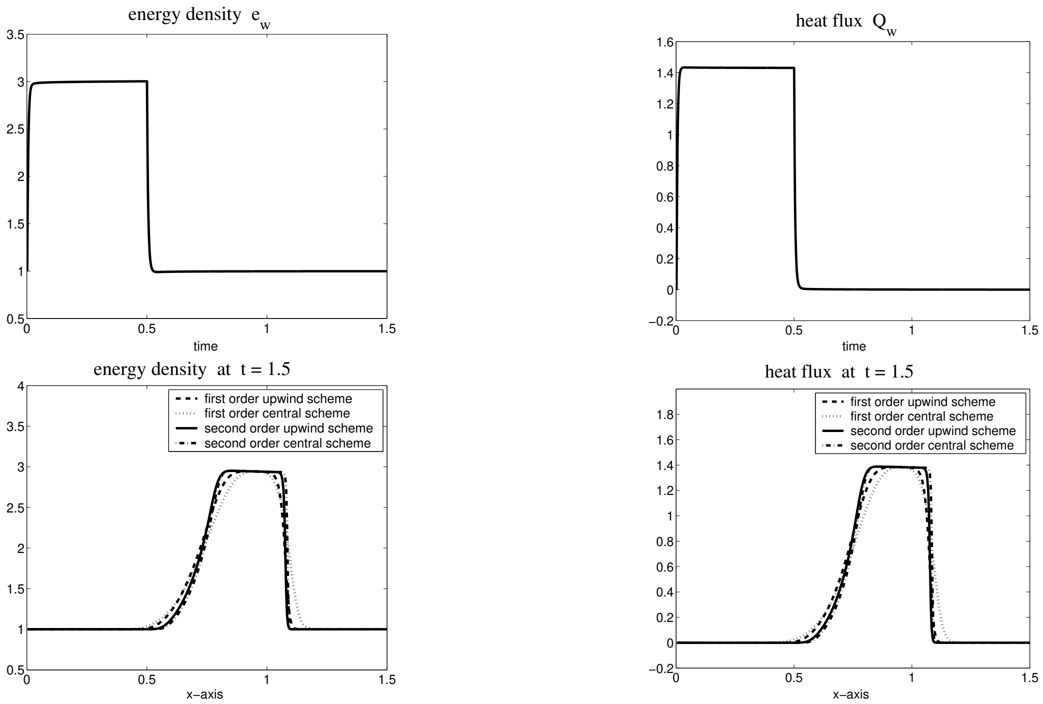

Figure 11: Creation of heat pluse

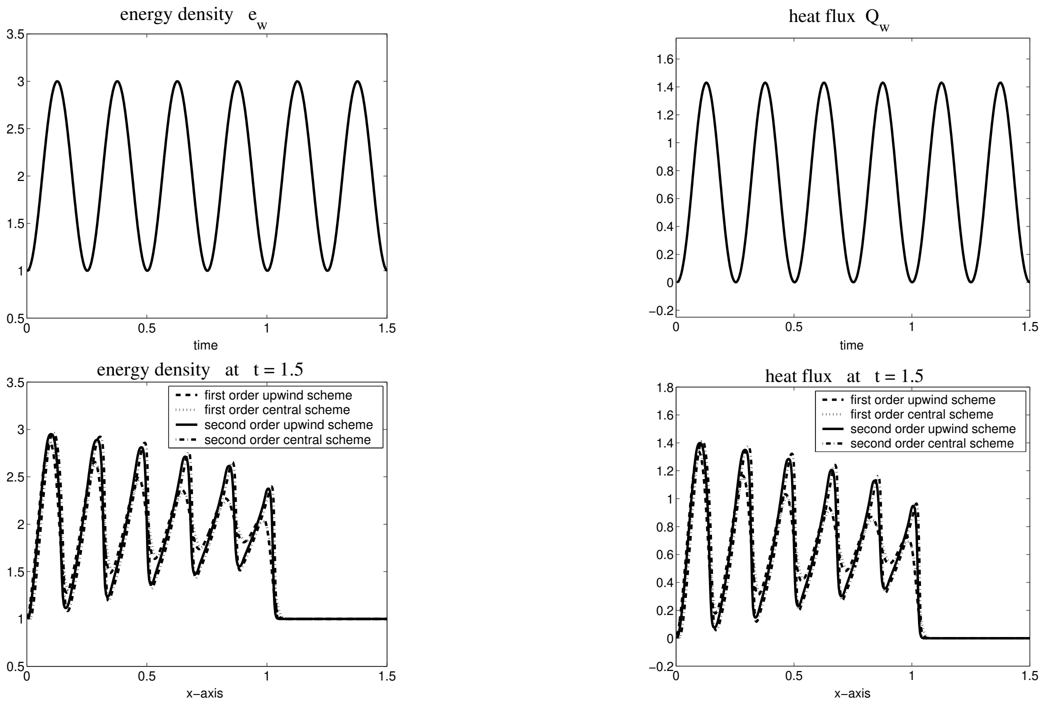

Figure 12: Periodic boundary conditions

References

[1] K. Aoki, K. Kanba, and S. Takata, "Numerical analysis of a supersonic rarefied gas flow past a flat plate", *Phys. Fluids*, **9**, pp. 1144-1161.

[2] G. Boillat, T. Ruggeri, "Moment equations in the kinetic theory of gases and wave velocities", *Cont. Mech. Thermodyn.,* **9**.**4**, (1996) pp. 175-195.

[3] C. Buet, "A discrete-velocity scheme for the Boltzmann operator of rarefied gas dynamics", *Transp. Th. Stat. Phys.* 25 (1994), pp. 313-338.

[4] J. Callaway, "Quantum theory of the solid state", Academic press, San Diego, 1991.

[5] W. Dreyer and M. Kunik, "Initial and boundary value problems of hyperbolic heat conduction", *Cont. Mech. Thermodyn.* **11.4** (1999) pp. 227-245.

[6] W. Dreyer, M. Herrmann and M. Kunik, "Kinetic solutions of the Boltzmann-Peierls equation and its moment systems", *WIAS-Preprint* No. **709**, Berlin (2001).

[7] W. Dreyer, S. Seelecke, "Entropy and causality as criteria for the existence of shock waves in low temperature heat conduction", *Cont. Mech. Thermodyn.,* **4**, (1992) pp. 23-36.

[8] W. Dreyer, H. Struchtrup, "Heat pulse experiments revisited", *Cont. Mech. Thermodyn.,* **5**, (1993) pp. 1-50.

[9] R. Gatignol, "Théorie cinétique des gaz á répartition discréte de vitesses", Lecture Notes in Physics **36**, Speringer-Verlag, 1975.

[10] D. Issautier, "Convergence of a weighted particle method for solving the Boltzmann (B.G.K.) equation", *SIAM J. Numer. Anal.* **33**, (1996), pp.2099-2119.

[11] G.-S. Jaing , E. Tadmor, "non-oscillatory central schemes for multidimensional hyperbolic conservation laws", *SIAM J. Sci. Comput.* **19**, (1998), pp. 1892-1917.

[12] M. Kunik, S. Qamar and G. Warnecke, "Kinetic schemes for the ultra-relativistic Euler equations", *J. Comput. Phys.* **187**, (2003), pp. 572-596.

[13] M. Kunik, S. Qamar and G. Warnecke, "A BGK-type kinetic flux-vector splitting schemes for the ultra-relativistic relativistic gas dynamics", Preprint Nr. **4**, Otto-von-Guericke University, (2003).

[14] M. Kunik, S. Qamar and G. Warnecke, "A reduction of the Boltzmann-Peierls equation", Preprint Nr. **6**, Otto-von-Guericke University, (2003).

[15] M. Kunik, S. Qamar and G. Warnecke, "Second order accurate kinetic schemes for the ultra-relativistic Euler equations", Preprint Nr. **18**, Otto-von-Guericke University, (2003).

[16] S.F. Liotta, V.R. Romano and G. Russo, “Central schemes for balance laws of relaxation type”, *SIAM J. Numer. Anal.* 38 (2000), pp. 1337-1356.

[17] L. Mieussens, “discrete-velocity model and implicit scheme for the BGK equation of rarefied gas dynamics”, *Mathematical Models of Methods in Applied Sciences*, **8**, (2000), pp. 1121-1149.

[18] H. Nessayahu, E. Tadmor, “Non-oscillatory central differencing fo hyperbolic conservation Laws”,*SIAM J. Comput. Phys.* **87**, (1990), pp. 408-448.

[19] R.E. Peierls, “Quantum theory of solids”, Oxford University press, London 1995.

[20] B. Perthame, “Boltzmann type schemes for gas dynamics and the entropy property”, *SIAM J.Numer.Anal.* **27.6** (1990) pp. 1405-1421.

[21] F. Rogier and J. Schneider, “A direct method for solving the Boltzmann equation”, *Transp. Th. Stat. Phys.* 23 (1994), pp. 313-338.

[22] E.F. Toro, “Riemann solvers and numerical method for fluid dynamics”, Second Edition, Springer-Verlag, (1999).

[23] J.Y. Yang and J.C. Huang, “Rarefied flow computations using nonlinear nodel Boltzmann equation”, *J. Comput. Phys.* **120**, (1995), pp. 323-339.